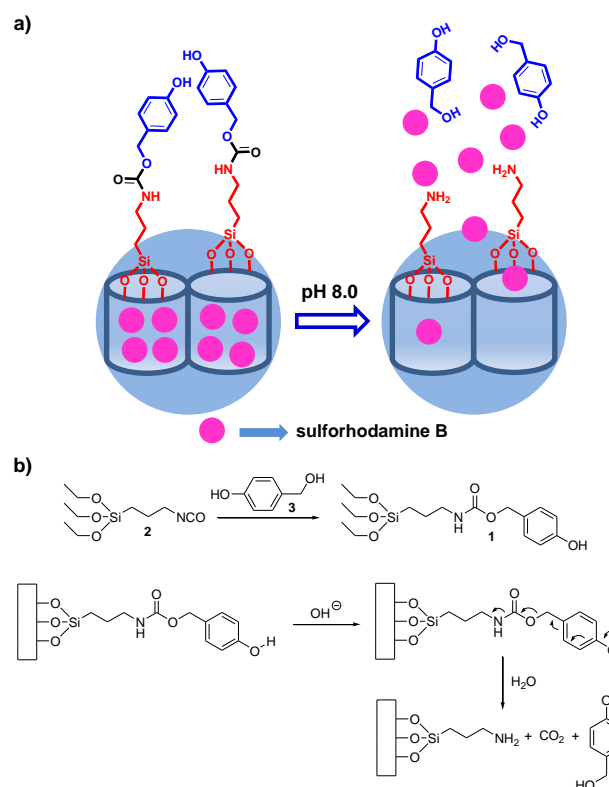


**Abstract:** Synthesis, characterization and controlled release behavior of a new hybrid material based on silica mesoporous nanoparticles capped with a self-immolative gate is reported.

There is a significant interest in the development of methodologies of controlled release for a diverse range of applications.<sup>[1]</sup> For this reason, a large diversity of drug nanocarriers having different size, structure and surface properties, such as liposomes and polymeric or inorganic nanoparticles, have been developed over the last decades.<sup>[2]</sup> Among these, mesoporous silica nanoparticles (MSNs) have attracted great attention in recent years due to their unique features such as stability, biocompatibility, large load capacity and the possibility of easy functionalizing their surface to obtain targeting and drug release systems.<sup>[3]</sup> In this scenario, an appealing concept when using MSNs is the possibility to functionalize the external surface with gated ensembles. The development of gated systems able to retain the payload yet releasing it upon the presence of a predefined stimulus has been proved to be an excellent approach to develop advanced nanodevices for controlled delivery applications.<sup>[4]</sup> In fact, through decoration of the mesoporous material with a wide collection of organic and biological entities or inorganic capping agents, researchers have prepared recently gated MSNs that can be triggered by target chemical (such as selected anions, cations neutral molecules, redox-active molecules, pH changes and biomolecules), physical (such as light, temperature, magnetic fields or ultrasounds) and biochemical (such as enzymes, antibodies, or DNA) stimuli.<sup>[5]</sup>

From a different point of view, self-immolative molecules are covalent aggregates that, upon application of an external trigger, initiate a disassembly reaction, through a cascade of electronic elimination processes, leading ultimately to the release of its building blocks.<sup>[6]</sup> This chemical phenomenon is usually driven by a cooperative increase in entropy coupled with the irreversible formation of thermodynamically stable products. These molecules have been extensively used in several applications including the design of prodrugs,<sup>[7]</sup> sensors<sup>[8]</sup> and drug delivery systems.<sup>[9]</sup> Self-immolative processes can commonly be found for polysubstituted, electron-rich aromatic

species containing an electron-donating substituent in conjugation (ortho or para) with a suitable leaving group located in a benzylic position.<sup>[10]</sup> In classical self-immolative linkers a single activation event leads to the release of a single group. This release can be described as non-amplified. In contrast the evolution of this technology has resulted in recent years in the design of self-immolative systems in which a single activation event leads to the delivery of multiple groups. This has been described as amplified release.<sup>[11]</sup>



**Scheme 1.** (a) Schematic representation of the prepared gated nanoparticles S1, (b) synthesis of self-immolative molecular gate 1 and the cascade electronic elimination reaction triggered by pH.

Taking into account our interest in the preparation of capped mesoporous materials for applications in controlled release<sup>[12]</sup> and sensing/recognition<sup>[13]</sup> protocols we describe herein the possibility of combining MSNs and self-immolative derivatives in order to develop new gated MSNs supports. In this context, and as far as we are aware, the use of self-immolative molecules as caps in conjunction with mesoporous supports for the preparation of gated nanodevices has never been described. The design of our system is shown in Scheme 1. MCM-41 mesoporous silica nanoparticles of ca. 100 nm of diameter were selected as inorganic scaffold and were loaded with the dye sulforhodamine B. As cap we selected the simple molecule 1 in order to demonstrate that it is possible to use self-immolative linkers to prepare gated MSNs. 1 is a carbamate derivative that can suffer a 1,6 elimination reaction via a quinone-methide cascade under basic conditions (see Scheme 1).

[a] Instituto Interuniversitario de Investigación de Reconocimiento Molecular y Desarrollo Tecnológico (IDM). Unidad Mixta Universidad de Valencia-Universidad Politécnica de Valencia, Spain.

[b] L. A. Juárez, E. Añón, A. M. Costero, P. Gaviña Departamento de Química Orgánica. Universidad de Valencia, Doctor Moliner 50, 46100, Burjassot, Valencia, Spain. E-mail: ana.costero@uv.es

[c] C. Gimenez, F. Sancenón, R. Martínez-Mañez Departamento de Química. Universidad Politécnica de Valencia, Camino de Vera s/n, 46022, Valencia, Spain.

[d] CIBER de Bioingeniería Biomateriales y Nanomedicina (CIBER-BBN).

The self-immolative molecule **1** was prepared by simple reaction of (3-isocyanatopropyl)triethoxysilane (**2**) with 4-hydroxymethylphenol (**3**) (see Scheme 1). On the other hand, MSNs were prepared following well-known procedures using tetraethyl orthosilicate (TEOS), as suitable hydrolysable inorganic precursor, and hexadecyltrimethylammonium bromide (CTAB) as a structure-directing agent.<sup>[14]</sup> The preparation of the final **S1** material was carried out using a two-step procedure. In a first step, the pores of the calcined mesoporous scaffold were loaded with sulforhodamine B by simply stirring a suspension of the nanoparticles in a concentrated acetonitrile solution of the dye. In the second step, self-immolative molecule **1** was added to the suspension. Using this protocol **1** was expected to be preferentially attached onto the external surface of the nanoparticles due to the presence of the sulforhodamine B dye inside the pores. After the grafting step, the nanoparticles were filtered, washed with acetonitrile and dried at 70°C for 12 h. This procedure yielded the final **S1** material as a red-pink solid.

The starting mesoporous silica scaffold and the final nanoparticles **S1** were characterized following standard procedures (see Supporting Information for details). Powder X-ray diffraction (PXRD) and transmission electron microscopy (TEM), carried out on the starting nanoparticles showed the presence of a mesoporous structure (see Figures 1 and 2). Figure 1 shows the PXRD pattern of the as-made mesoporous nanoparticles (curve a), the calcined solid (curve b) and the final material **S1** (curve c). As it could be seen, the (100) reflection was present in the three patterns indicating the preservation of the mesoporous scaffolds. The presence of the mesoporous structure on the final functionalized solid **S1** was also confirmed by TEM. Figure 2 shows the pseudo-spherical morphology of the obtained materials and the typical channels of the MCM-41 matrix visualized as a pseudo-hexagonal array of pore voids or as alternate black and white strips. The prepared final MSNs **S1** have a diameter of  $94 \pm 5$  nm (Figure 2).

N<sub>2</sub> adsorption-desorption isotherms studies of the starting calcined nanoparticles and of the final material **S1** were also performed (see Supporting Information). The curve of calcined nanoparticles showed an absorption step at P/P<sub>0</sub> values between 0.1 and 0.3 (type IV isotherm) which is typical of mesoporous solids. This first step is attributed to N<sub>2</sub> condensation inside the mesopores. Application of the BJH model on the adsorption curve of the isotherm, pore diameter and pore volume were calculated (see Table 1). The absence of a hysteresis loop within this range and the low BJH distribution suggest a cylindrical uniformity of the mesopores. Applying the BET model, a total specific surface area of 895 m<sup>2</sup> g<sup>-1</sup> was calculated. A second characteristic of the isotherm of the starting calcined nanoparticles is the characteristic H1 hysteresis loop that appeared at P/P<sub>0</sub> > 0.8 and corresponding to the filling of the large pores between nanoparticles attributed to textural porosity. For the final capped nanoparticles **S1**, the N<sub>2</sub> adsorption-desorption isotherm (see Supporting Information) is typical of mesoporous systems with partially filled mesopores. As expected, smaller pore volume and specific surface area were found for **S1** (see Table 1), when compared with the starting MSNs. Finally, elemental and thermogravimetric analyses were used to determine the organic content in the final

gated nanoparticles **S1**. The content of **1** and sulforhodamine B amounted to 0.107 and 0.39 mmol g<sup>-1</sup> SiO<sub>2</sub>, respectively.

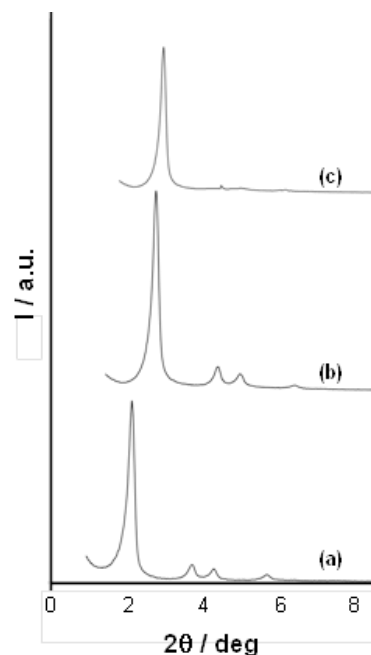


**Figure 1.** Powder X-ray patterns of the solids: (a) MCM-41 as synthesized, (b) calcined MCM-41, (c) **S1** nanoparticles.

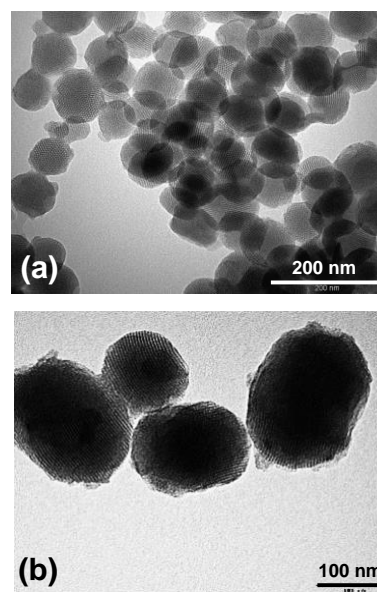


**Figure 2.** TEM images of (a) calcined MCM-41, (b) **S1** nanoparticles. For all the materials, the typical porosity of the mesoporous matrix is observed.

**Table 1.** BET specific surface values, pore volumes and pore sizes calculated from the N<sub>2</sub> adsorption-desorption isotherms for calcined MSNs and **S1**.

Solid	S <sub>BET</sub> (m <sup>2</sup> g <sup>-1</sup> )	Pore volume (cm <sup>3</sup> g <sup>-1</sup> ) <sup>[a]</sup>	Pore size (nm) <sup>[b]</sup>
calcined MSNs	895	0.73	2.47
<b>S1</b>	265	0.35	2.45

[a] Pore volumes and pore sizes were associated with only intraparticle mesopores. [b] Pore sizes estimated by the BJH model applied to the absorption branch of the isotherm.

**S1** nanoparticles contain phenolic carbamate groups as self-immolative caps. Taking into account the content of **1** (0.107 mmol g<sup>-1</sup> SiO<sub>2</sub>) in **S1** solid and according to a typical external surface for the MCM-41 nanoparticles of ca. 70 m<sup>2</sup> g<sup>-1</sup>, the average surface coverage on the final capped material amounts to ca. 0.92 molecules nm<sup>-2</sup>. This surface coverage resulted in an average distance between **1** molecules of about 10.4 Å. Additionally, bearing in mind the nanoparticle diameter (ca. 100 nm) and its average surface coverage (in molecules nm<sup>-2</sup>) each nanoparticle was functionalized with ca. 29000 molecules of **1**. The high surface coverage value indicated the formation of a dense hydrogen-bonded monolayer of compound **1** around pore outlets that inhibited sulforhodamine B release. However, deprotonation of the phenolic hydroxyl group is expected to result in cargo delivery. In fact taking into account the designed opening protocol (vide ante), it was anticipated that at pH below the pK<sub>a</sub> of the phenolic subunit in **1** (pK<sub>a</sub> ca. 9-10) the nanoparticles **S1** would remain closed. However, at basic pH the deprotonation of the hydroxyl would result in a cascade disassembly reaction and cargo delivery. In order to test this designed aperture mechanism kinetic cargo release profiles for solid **S1** at different pH values were obtained. In a typical experiment 1.0 mg of the solid **S1** was suspended in water at pH 4.0, 5.0, 7.5 or 8.0. Mixtures were stirred at room temperature and aliquots were taken at scheduled times. The solid was then removed by centrifugation and the dye delivered to the solution was monitored by measuring the emission of sulforhodamine B in the solution at λ = 560 nm (λ<sub>ex</sub> = 550 nm), provided that both absorption and emission spectra of sulforhodamine B are independent on pH.<sup>[14]</sup> The results of cargo delivery as a function of the pH are shown in Figure 3.

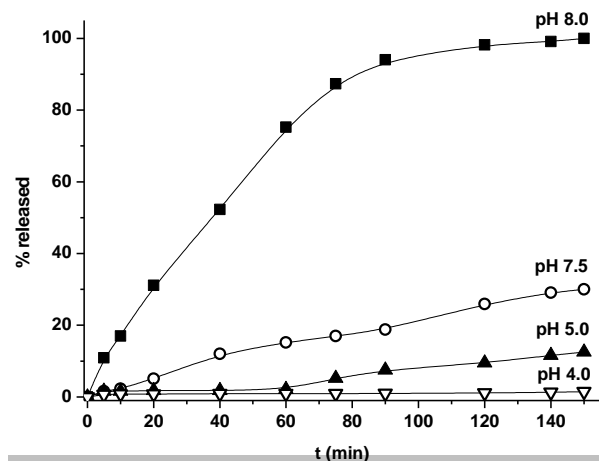


**Figure 3.** Release kinetic profiles of sulforhodamine B (emission at 560 nm upon excitation at 525 nm) from **S1** nanoparticles at different pH values (100% of release represent the total amount of dye delivered from solid **S1** after 150 min).

As seen, at pH 4.0, despite the use of a rather small molecule such as **1** anchored in the pore outlets, delivery of sulforhodamine B from the pores of **S1** nanoparticles was highly inhibited and a near “zero release” was observed. Nearly the same behavior was found when the pH was raised to 5.0 where the % of dye released was less than ca 10% after 5h. At pH 7.5 still a relatively low dye delivery was found (ca. 30% after 5h), whereas sulforhodamine B release was highly enhanced at pH 8.0 reaching the maximum cargo delivery at ca. 120 minutes. As expected (vide ante) the observed cargo release at basic pH was ascribed to a deprotonation of the hydroxyl moiety of **1**. The generated phenolate anion initiated a self-immolative process that induced the rupture of the gate with and the subsequent dye release (see Scheme 1). Delivery experiments at more basic pH were not carried out because of possible degradation of the inorganic mesoporous matrix. The autonomous disassembly of the self-immolative cap upon deprotonation of the phenolic hydroxyl moiety was assessed by means of <sup>1</sup>H NMR spectra and by HRMS. For this purpose, a suspension of **S1** in water at pH 8.0 was stirred at room temperature for 3 hours. The nanoparticles were removed by centrifugation. The resulting solution rotavapored and the obtained crude dissolved in deuterated acetonitrile. The <sup>1</sup>H-NMR spectrum of the crude clearly showed the presence of signals corresponding to 4-hydroxymethylphenol which was generated by reaction of the elimination product *p*-quinone methide with water (see Scheme 1). In contrast, signals of 4-hydroxymethylphenol were not observed if **S1** was suspended in water at acidic pH. The presence of the 4-hydroxymethylphenol derivative unequivocally confirms the occurrence of a disassembly reaction of the self-immolative gate at basic pH in **S1**.

As stated above in classical self-immolative chemistry a single activation event usually leads to the release of a single group whereas the design of self-immolative systems for the delivery of multiple groups is usually difficult and requires the preparation of rather complex challenging molecules from a synthesis point of view.<sup>[15]</sup> In this scenario, the anchoring as cap of a simple molecule such as **1** in MSNs allows to design systems in which a single activation in **1** induced the release of a large number of cargo molecules (in our case a dye). In fact, one reported advantage of gated materials is the existence of amplification features. For instance, it has been described that the “activation” of relatively few capping molecules usually results in the release of a relatively large quantity of entrapped cargo guests.<sup>[16]</sup> The approach of using self-immolative molecules as gates offers great potential for the preparation of new delivery systems with enhanced features compared with classical self-immolative systems for delivery applications. In particular, it is possible to select, with minimum effort, different

porous supports, a large range of self-immolative gate-like systems and a number of molecules to be delivered which do not need to be anchored to the self-immolative linker. In fact, this approach is conceptually different to classic self-immolative showing molecular amplification because our proposed protocol disconnects the triggering step from the release event therefore making delivery independent of the interaction between the activation event and the self-immolative linker.

In summary, we reported herein the synthesis, characterization and pH-triggered controlled release behavior of a new hybrid material based on silica mesoporous nanoparticles loaded with sulforhodamine B and capped with a self-immolative cap. At acidic and neutral pH the gate remained closed and negligible or poor dye release was observed. However, at slightly basic pH a marked cargo delivery was observed. Dye release was ascribed to a deprotonation of the phenol moiety in the capping molecule that resulted in the subsequent disassembly of the self-immolative cap. As far as we know, this is the first example in which a self-immolative molecule is used as cap for the development of mesoporous silica-based gated materials. Self-immolative linkers have gained popularity in recent years due to the formation of stable bonds which become labile upon activation. We believe that the combination of self-immolative linkers with mesoporous materials could result in the easy preparation of a new generation of self-immolative systems. Moreover, the possibility to design capped self-immolative supports able to be opened by using pH, specific enzymes, small molecules, etc. makes this approach highly attractive for the preparation of new gated self-immolative systems for different applications.

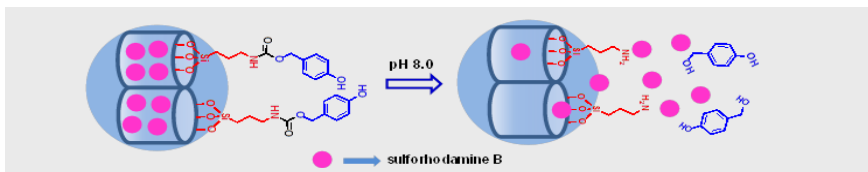
## Acknowledgements

We thank the Spanish Government and FEDER funds (MAT2015-64139-C4-1-R and MAT2015-64139-C4-4-R) and Generalitat Valenciana (PROMETEOII/2014/047) for support. SCSIE (Universidad de Valencia) is gratefully acknowledged for all the equipment employed.

**Keywords:** self-immolative gate • mesoporous silica nanoparticles • pH

- [1] a) M. W. Tibbit, J. E. Dahlman, R. Langer, *J. Am. Chem. Soc.* **2016**, *138*, 714; b) K. Nguyen, T. Kim, Y. Zhao, *Acc. Chem. Res.* **2015**, *48*, 3016; c) G. Kang, N. Tripathy, *Ther. Deliv.* **2014**, *5*, 1053.
- [2] a) N. Kamaly, B. Yameen, J. Wu, O. C. Farokhzad, *Chem. Rev.* **2016**, *116*, 2602; b) Y. Li, G. Liu, X. Wang, J. Hu, S. Liu, *Angew. Chem. Int. Ed.* **2016**, *55*, 1760; c) N. Sharma, K. Neeraj, V. Kumar, *Drug Deliv. Lett.* **2014**, *4*, 12; d) I. K. Yazdi, A. Ziemys, M. Evangelopoulos, J. O. Martinez, M. Kojic, E. Tasciotti, *Nanomedicine* **2015**, *10*, 3057.
- [3] a) C. Argyo, V. Weiss, C. Bräuchle, T. Bein, *Chem. Mater.* **2014**, *26*, 435; b) J. El Haskouri, D. Ortiz de Zarate, C. Guillem, J. Latorre, M. Caldés, A. Beltrán, D. Beltrán, A. B. Descalzo, G. Rodríguez-López, R. Martínez-Mañez, M. D. Marcos, P. Amorós, *Chem. Commun.* **2002**, 330.
- [4] a) G. J. A. A. Soler-Illia, O. Azzaroni, *Chem. Soc. Rev.* **2011**, *40*, 1107; b) N. Song, Y. -W. Yang, *Chem. Soc. Rev.* **2015**, *44*, 3474; c) E. Aznar, R. Martínez-Mañez, F. Sancenón, *Expert Opin. Drug Deliv.* **2009**, *6*, 643; d) C. Coll, A. Bernardos, R. Martínez-Mañez, F. Sancenón, *Acc. Chem. Res.* **2013**, *46*, 339.
- [5] See for example: a) E. Aznar, M. Oroval, L. Pascual, J. R. Murguía, R. Martínez-Mañez, F. Sancenón, *Chem. Rev.* **2016**, *116*, 961; b) F. Sancenón, L. Pascual, M. Oroval, E. Aznar, R. Martínez-Mañez, *Chemistry Open* **2015**, *4*, 418; c) Z. Li, J. C. Barnes, A. Bosoy, J. F. Stoddart, J. I. Zink, *Chem. Soc. Rev.* **2012**, *41*, 2590; d) C. -H. Lu, B. Willner, I. Willner, *ACS Nano* **2013**, *7*, 8320; e) S. Saha, K. C. -F. Leung, T. D. Nguyen, J. F. Stoddart, J. I. Zink, *Adv. Func. Mater.* **2007**, *17*, 685; f) B. G. Trewyn, I. I. Slowing, S. Giri, H. -T. Chen, V. S. -Y. Lin, *Acc. Chem. Res.* **2007**, *40*, 846; g) Y. -W. Yang, Y. -L. Sun, N. Song, *Acc. Chem. Res.* **2014**, *47*, 1959; h) F. Tang, L. Li, D. Chen, *Adv. Mater.* **2012**, *24*, 1504; i) C. -H. Lu, I. Willner, *Angew. Chem. Int. Ed.* **2015**, *54*, 12212; j) C. Argyo, V. Weiss, C. Bräuchle, T. Bein, *Chem. Mater.* **2014**, *26*, 435; k) P. Yang, S. Gai, J. Lin, *Chem. Soc. Rev.* **2012**, *41*, 3679; l) N. Song, Y. -W. Yang, *Chem. Soc. Rev.* **2015**, *44*, 3474; m) A. Bansal, Y. Zhang, *Acc. Chem. Res.* **2014**, *47*, 3052; n) S. Mura, J. Nicolas, P. Couvreur, *Nat. Mater.* **2013**, *12*, 991; o) V. Z. Ozalp, F. Eyidogan, H. A. Oktem, *Pharmaceuticals* **2011**, *4*, 1137; p) R. de la Rica, D. Aili, M. M. Stevens, *Adv. Drug Delivery Rev.* **2012**, *64*, 967; q) S. Alberti, G. J. A. A. Soler-Illia, O. Azzaroni, *Chem. Commun.* **2015**, 51, 6050.
- [6] a) A. Alouane, R. Labruère, T. Le Saux, F. Schmidt, L. Jullien, *Angew. Chem. Int. Ed.* **2015**, *54*, 7492; (b) S. Gnaïm, D. Shabat, *Acc. Chem. Res.* **2014**, *47*, 2970.
- [7] See for example: a) H. J. Schuster, B. Krewer, J. M. von Hof, K. Schmuck, I. Schubert, F. Alves, L. F. Tietze, *Org. Biomol. Chem.* **2010**, *8*, 1833; b) B. E. Toki, C. G. Cervený, A. F. Wahl, D. Seuter, *J. Org. Chem.* **2002**, *67*, 1866; c) S. Chen, X. Zhao, J. Chen, J. Chen, L. Kuznetsova, S. S. Wong, I. Ojima, *Bioconjugate Chem.* **2010**, *21*, 979.
- [8] See for example: a) L. Louise-Leriche, E. Paunescu, G. Saint-Anfre, R. Baati, A. Romieu, A. Wagner, P. Y. Renard, *Chem. Eur. J.* **2010**, *16*, 3510; b) Y. Meyer, J. A. Richard, M. Massonneau, P. Y. Renard, A. Romien, *Org. Lett.* **2008**, *10*, 1517; c) X. B. Zhang, M. Waibel, J. Hasserodt, *Chem. Eur. J.* **2010**, *16*, 792.
- [9] See for example: a) A. Satyam, *Bioorg. Med. Chem. Lett.* **2008**, *18*, 3196; b) M. Shamis, H. N. Lode, D. Shabat, *J. Am. Chem. Soc.* **2004**, *126*, 1726; c) R. Weinstein, E. Segal, R. Satchi-Fainaro, D. Shabat, *Chem. Commun.* **2010**, 46, 533; d) R. J. Amir, M. Popkov, R. A. Lernes, C. F. Barbas III, D. Shabat, *Angew. Chem. Int. Ed.* **2005**, *44*, 4378.
- [10] a) H. Y. Lee, X. Jiang, D. Lee, *Org. Lett.* **2009**, *11*, 2065; b) A. Alouane, R. Labruère, T. Le Saux, I. Aujard, S. Dubrulle, F. Schmidt, L. Jullien, *Chem. Eur. J.* **2013**, *19*, 11717; c) R. Erez, D. Shabat, *Org. Biomol. Chem.* **2008**, *6*, 2669; d) R. M. Kewitch, C. S. Shanahan, D. V. McGrath, *New. J. Chem.* **2012**, *35*, 492.
- [11] a) M. E. Roth, O. Green, S. Gnaïm, D. Shabat, *Chem. Rev.* **2016**, *116*, 1309; b) G. Liu, G. Zhang, J. Hu, X. Wang, M. Zhu, S. Liu, *J. Am. Chem. Soc.* **2015**, *137*, 11645; c) I. S. Turan, E. U. Akkaya, *Org. Lett.* **2014**, *16*, 1680; d) N. Fomina, C. L. McFearn, A. Almutairi, *Chem. Commun.* **2012**, *48*, 9138.
- [12] See for example: a) A. Ultimo, C. Giménez, P. Bartovsky, E. Aznar, F. Sancenón, M. D. Marcos, P. Amorós, A. R. Bernardo, R. Martínez-Mañez, A. M. Jiménez-Lara, J. R. Murguía, *Chem. Eur. J.* **2016**, *22*, 1582; b) C. de la Torre, I. Casanova, G. Acosta, C. Coll, M. J. Moreno, F. Albericio, E. Aznar, R. Mangués, M. Royo, F. Sancenón, R. Martínez-Mañez, *Adv. Func. Mater.* **2015**, *25*, 687; c) C. de la Torre, L. Modragón, C. Coll, A. García-Fernández, F. Sancenón, R. Martínez-Mañez, P. Amorós, E. Pérez-Payá, M. Orzaez, *Chem. Eur. J.* **2015**, *21*, 15506; d) N. Mas, D. Arcos, L. Polo, E. Aznar, S. Sánchez-Salcedo, F. Sancenón, A. García, M. D. Marcos, A. Baeza, M. Vallet-Regí, R. Martínez-Mañez, *Small* **2014**, *23*, 4859.
- [13] See for example: a) L. Pascual, I. Baroja, E. Aznar, F. Sancenón, M. D. Marcos, J. R. Murguía, P. Amorós, K. Ruck, *Chem. Commun.* **2015**, 51, 1414; b) S. El Sayed, M. Milani, M. Licchelli, R. Martínez-Mañez, F. Sancenón, *Chem. Eur. J.* **2015**, *21*, 7002; c) E. Climent, L. Modragón, R. Martínez-Mañez, F. Sancenón, M. D. Marcos, J. R. Murguía, P.

- 
- Amorós, K. Rurack, E. Pérez-Payá, *Angew. Chem. Int. Ed.* **2013**, *52*, 8938.
- [14] J. Coppeta, C. Rogers, *Experiments in Fluids* **1998**, *25*, 1
- [15] S. Cabrera, J. El Haskouri, C. Guillem, J. Latorre, A. Beltrán, D. Beltrán, M.D- Marcos, P. Amorós, *Solid State Sci.* **2000**, *2*, 405.
- [16] E. Climent, M. D. Marcos, R. Martínez-Máñez, F. Sancenón, J. Soto, K. Rurack, P. Amorós, *Angew. Chem. Int. Ed.* **2009**, *48*, 8519.
-



Synthesis, characterization and controlled release behavior of a new hybrid material based on silica mesoporous nanoparticles capped with a self-immolative gate is reported.

*L. Alberto Juárez, Elena Añón, Cristina Giménez, Félix Sancenón, Ramón Martínez-Máñez,\* Ana M. Costero,\* Pablo Gaviña, Margarita Parra.*

**Page No. – Page No.**

**Self-immolative linkers as caps for the design of gated silica mesoporous supports**